Available online at www.sciencedirect.com

ScienceDirect

Procedia Engineering 66 (2013) 88 – 97

Procedia Engineering

www.elsevier.com/locate/procedia

5th Fatigue Design Conference, Fatigue Design 2013

Fatigue tests of axially loaded butt welds up to very high cycles

P. Schaumann, S. Steppeler*

Institute for Steel Construction, Leibniz Universitaet Hannover, Appelstrasse 9A, 30167 Hannover, Germany

Abstract

Fatigue strength curves that are established from fatigue tests provide a basis for the fatigue assessment applying nominal stress approach. In the codes valid for steel structures, like the EC 3, the fatigue strength curves for constant amplitude loading have a knee point in the transition region. The fatigue strength curve beyond this knee point is commonly assumed to be a horizontal asymptote. However, the behaviour of the fatigue strength curve in the area of very high cycles and more importantly the existence of an endurance limit are much discussed. In the case of welded joints the experimental data beyond 10^7 load cycles is limited due to the possibilities in testing. Testing techniques with high frequencies are necessary to obtain experimental data with very high cycles in a reasonable period of time. In this scope a testing device with approximately 390 Hz operates by alternating current magnets and using resonance amplification, which was developed by a third party. This testing device was investigated and advanced for the application of long term tests reaching $5 \cdot 10^8$ load cycles. Fatigue tests on axially loaded butt welds with constant amplitude loading are conducted in three test series until very high cycles. The fatigue tests include the area of high and very high cycles. The influence of test frequency and stress ratio is investigated.

Keywords: Welded joints; Steel; SN-curves; Very high cylce fatigue; Test frequency; Stress ratio

1. Introduction

The fatigue assessment of steel structures is generally performed according to valid codes, like the EC 3 [1] and the recommendations of the International Institute of Welding (IIW) [2]. Fatigue strength curves (SN-curves) based on fatigue tests provide a basis for the fatigue assessment using nominal stress approach. In reference to the codes for steel structures the transition region of the constant amplitude fatigue limit is defined at $5 \cdot 10^6$ respectively 10^7 load cycles. Beyond this knee point the SN-curve is commonly assumed to be a horizontal asymptote under constant

* Corresponding author. Tel.: +49-511-762-17212; fax: +49-511-762-2991.
E-mail address: steppeler@stahl.uni-hannover.de

doi:10.1016/j.proeng.2013.12.065

amplitude loading as illustrated in Fig. 1. Depending on the numbers of load cycles the SN-curve may be subdivided into three areas: Low Cycle Fatigue (LCF), High Cycle Fatigue (HCF) and Very High Cycle Fatigue (VHCF). The recommendations of IIW [2] have been updated [7]. According to the recommendations of IIW, the slopes of standard applications and very high cycle applications distinguishably diverge at 10^7 load cycles, as noted in Fig. 1. In the case of very high cycle applications a change in slope to m = 22 at 10^7 load cycles is recommended instead of a horizontal asymptote in the case of standard applications. In contrast, there is still a constant amplitude fatigue limit in EC 3 [1].

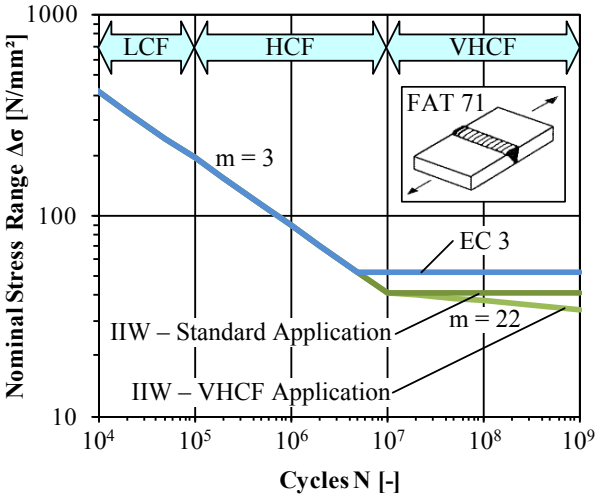

Fig. 1. SN-curve of FAT 71 of EC 3 [1] and IIW [2].

For welded joints the area of HCF ranging from 10^5 to 10^7 load cylces is well covered by fatigue tests. However, the course of the SN-curve in the VHCF area is subject to research. In particular, the existence of an endurance limit is of great interest, because several investigations on unwelded and welded components have shown that the fatigue strength may still decrease with increasing numbers of cycles [3,4]. Until now, basically unwelded metals with macroscopic homogeneous structures of unnotched components were investigated in the area of very high cycles under constant amplitude loading, which can be classified as less interesting for the assessment of components [5]. Fig. 2 shows that the experimental data of welded joints beyond 10^7 is limited [6]. This can be attributed to limited possibilities in testing. To obtain experimental data with very high cycles in a reasonable time frame, testing techniques with high frequencies are necessary.

The purpose of the research is to contribute to a safe fatigue design of welded joints in the area of very high cycles. Therefore, a testing device that operates by alternating current magnets and using resonance amplification is applied, which was developed by a third party. The test frequency is approximately 390 Hz in order to achieve acceptable testing time. This testing device was investigated and advanced for the application of long term tests reaching $5 \cdot 10^8$ load cycles and is presented in the following section. Fatigue tests with constant amplitude loading on axially loaded butt welds (S355J2+N, t = 4 mm) are conducted in three test series up to very high cycles. As a reference, one of the test series is carried out in a servo-hydraulic testing machine with 20 Hz. Two test series with different stress ratios are conducted in the presented testing device with approximately 390 Hz. The fatigue tests include the area of high and very high cycles. The influence of test frequency (20 Hz and 390 Hz) and stress ratio (R = 0.1 and R = 0.5) is investigated.

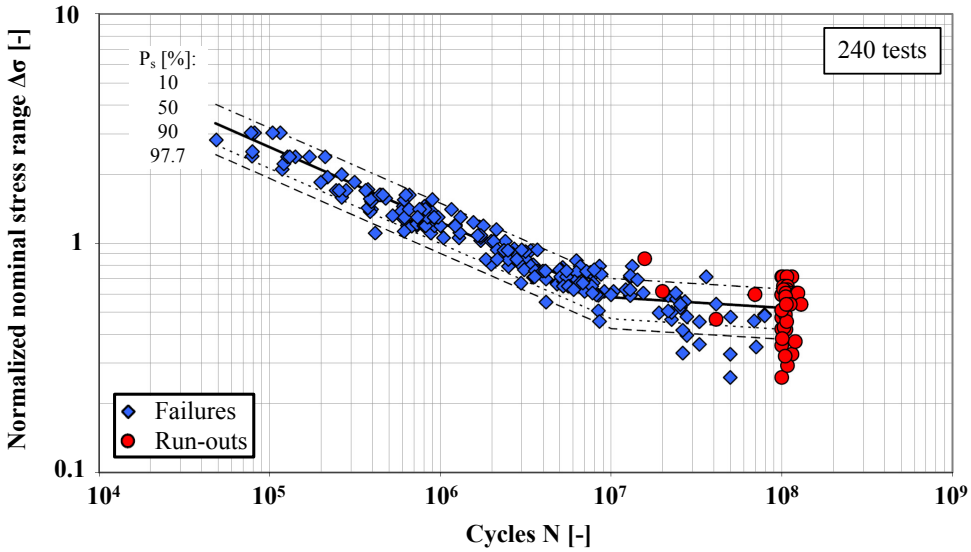

Fig. 2. Overview of normalized fatigue tests of weld joints from [6].

2. Experimental setup

2.1. Test equipment

The challenge in the experimental procedure is attaining an acceptable period of testing time in the area of VHCF. To conduct fatigue tests until very high cycles, testing machines with high frequencies are necessary. Conventional testing techniques in the area of HCF work with frequencies lower than 100 Hz. Besides individual developments, conventional servo-hydraulic or resonance fatigue testing machines may reach frequencies of 300 to 400 Hz depending on the experimental setup and test specimen size. Generally, ultrasonic testing machines working with frequencies up to 20 kHz are feasible for investigations in the area of VHCF. In case of welded components the production and testing of small non-distorted specimens needed for ultrasonic testing is deemed to be difficult [3]. Until now, the testing of components or component like specimens is not possible due to the special geometry of the specimen [4].

Based on a German patent [8], a testing device was developed operating by alternating current magnets and using resonance amplification. This testing device is not a universal testing machine. It is shaped and designed for special standardised specimens. Butt welds with a plate thickness up to 5 mm can be tested with a test frequency of approximately 390 Hz. The testing device allows testing with maximum load amplitude of 50 kN and maximum pretension force of 60 kN. For example, one test with 10^9 load cycles takes about 30 days.

Design and functional principle of the testing device are illustrated in Fig. 3. The bending part due to pretention of the specimen is neglected for reasons of simplification in the illustration of the functional principal. The resonance body has the shape of a closed rectangular frame. The long sides of the frame are extended at both ends each. The resonance body is bedded on the base plate at the corners of the frame. The alternating current magnets are mounted at the base plate at the extended ends of the frame, which allows for contact-free excitation using the magnets. The first natural frequency and related mode shape imply bending in opposite direction of the opposite frame sides. The test specimen is clamped between the long sides in the centre of the frame where the most bending takes place. Due to the symmetry of the first mode with respect to the axis of the test specimen the dynamic test load is purely axial. Four clamping blocks including two eccentric shafts allow for application of the preload. Due to the symmetry of the resonance body to the axis of the test specimen the preload is again purely axial. The nodal points

of the first mode are in the corners of the closed rectangular frame of the resonance body. These are the points at which the frame is supported in order to avoid dynamic reaction forces as well as vibration of the ground.

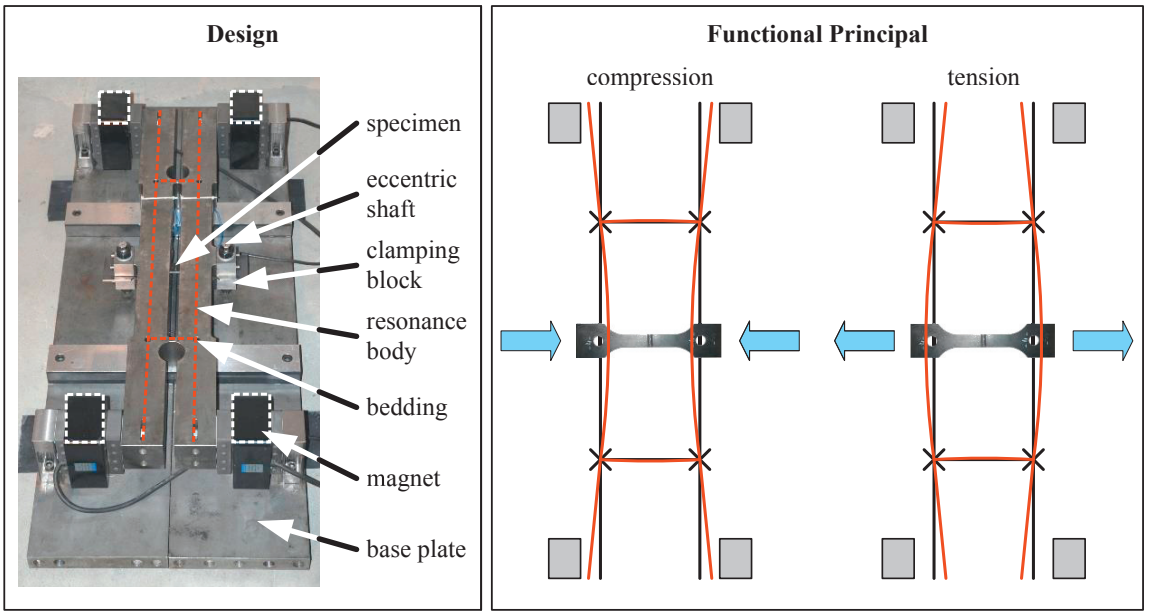

Fig. 3. Design and functional principal of testing device according to [8] and [9].

The testing device operates by alternating current magnets and using resonance amplification. The control loop of the testing device consists of resonance body, alternating current magnets, strain gauges, strain gauge amplifier, control unit and power amplifier. Strain gauges are applied at the outer and inner face of the resonance body. The control unit receives the electric signal of strain of the resonance body from the strain gauge amplifier as an input. The electromagnetic excitation of the resonance body results from the feedback of the signal of oscillation which is proportional to the loading of the specimen. The calibration of the signal is conducted by specimens with strain gauges. The control unit adjusts the measured signal with the set point and actuates the alternating current magnets with the power amplifier. For more details on the testing device and the control loop is referred to [8] and [9].

During the fatigue test time depended measurement data (test frequency, pretension force and load amplitude) is recorded with the software LabVIEW. The fatigue test is stopped when a defined number of cycles is reached (run-out) or the pretention force has decreased until a defined level (failure). The proportional relationship between the strain of the frame and the load of the specimen is valid until crack initiation. However, the fatigue test ends when the pretention force has decreased until a defined level where the specimen shows a significant crack. The determined number of cycles at the end of the fatigue test is not identical with the number of cycles of crack initiation. The number of cycles of crack initiation has to be evaluated from the time dependent measurement data. The time depended measurement data is displayed in Fig. 4 in case of failure. Test frequency, pretention force and load amplitude are plotted against the number of cycles. Towards the end of the fatigue test, the test frequency and the pretention force decrease exponentially. The crack grows through the cross section of the specimen and reduces the pretention force. Furthermore, the stiffness of the specimen and with it the test frequency is reduced. The test frequency was chosen as criterion for the determination of number of cycles of crack initiation. A decrease of 0.01 % of the test frequency from the linear regression line is defined as crack initiation as illustrated in Fig. 4.

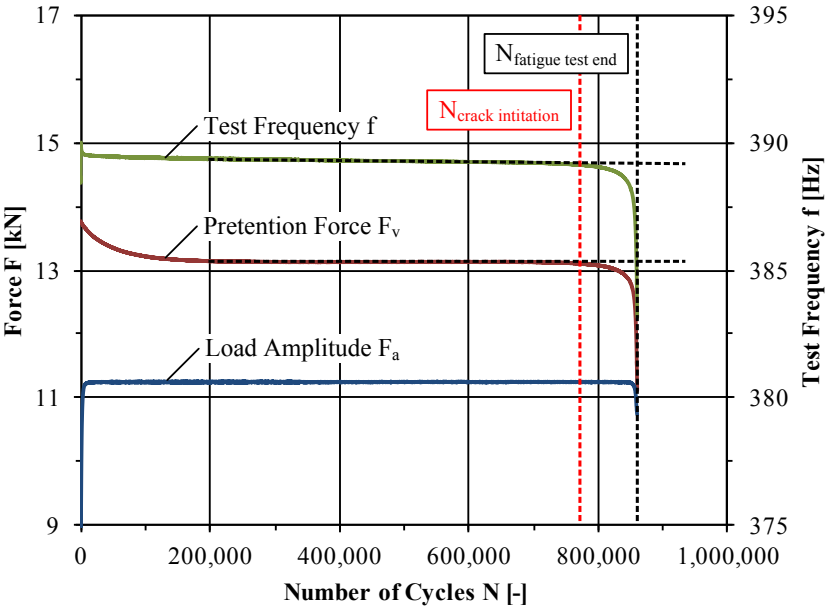

Fig. 4. Determination of number of cycles of crack initiation for time depended measurement data.

2.2. Test specimen

Steel plates of grade S355J2+N having the dimensions of 150 x 150 x 4 mm are joined by a MAG welding process with a one layer butt weld. Prior to welding, the steel plates were tack welded in the boundary area which is cut off later. The blowpipe guidance was mechanized by a welding tractor in order to achieve a high reproducibility of the manufactured specimens. The setup of the welding equipment consists of specimen bedding, blowpipe guidance and welding apparatus as shown in Fig. 5.

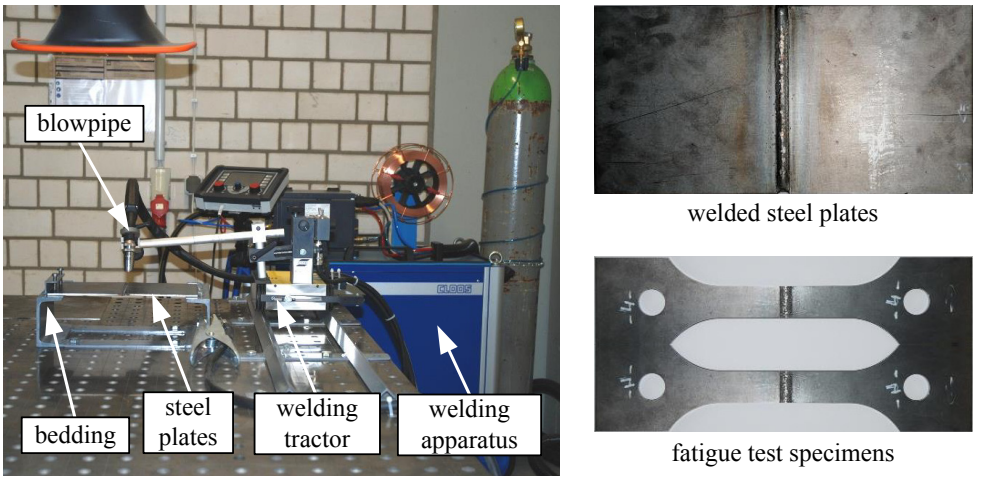

Fig. 5. Set up of the welding equipment (left) and welded steel plates and fatigue test specimen (right).

The bedding construction of the specimen and the guide rails of the welding tractor are fixed at a welding table. During the welding process the blowpipe is guided by the welding tractor across the tack welded steel plates with a constant speed. The tack welded steel plates were loose bedded on U-profiles during the welding process.

The specimens for the fatigue tests were cut from the welded steel plates by a milling cutter. The geometry of the specimen, shown in Fig. 6, is adapted to the special boundary conditions of the testing device described above. The weld is placed at the centre of the specimen. The overall dimension of the specimen is 300 x 70 mm. The specimen has a width of 25 mm in the testing cross section. Furthermore, there are two through holes at the ends of the specimen for fixing it in the testing device.

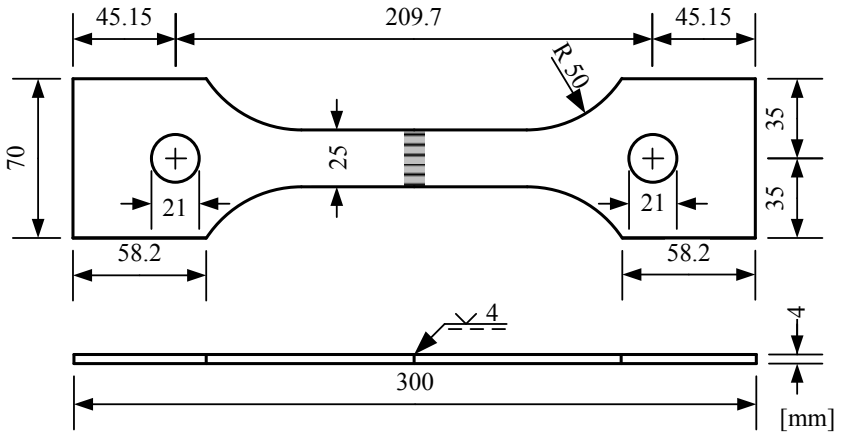

Fig. 6. Geometry of the fatigue test specimen.

The reproducibility of the welding process was evaluated by temperature measurements performed during the heating and cooling phase of the welding process. The quality of the welded specimens was proofed by determining the mechanical properties of base material and welded joint, metallurgical investigations and measurements of hardness. Furthermore, the execution quality B was checked by visual inspection according to DIN EN ISO 5817. For more details on the welding process and the evaluation of the reproducibility of the welding process and the quality of the welded specimens it is referred to [10].

2.3. Experimental agenda

In order to extend experimental investigations of welded joints in the VHCF area, fatigue tests on axially loaded butt welds are conducted in three test series (TS). The fatigue tests are performed at room temperature with constant amplitude loading in the as welded condition. Table I gives an overview of the experimental agenda.

Table 1. Experimental agenda.

Test Series	Test Equipment	Test Frequency f [Hz]	Stress Ratio R [-]	Number of tests
TS 1	servo-hydraulic	20	0.1	35
TS 2	developed testing device	390	0.1	28
TS 3	developed testing device	390	0.5	26

As a reference, TS 1 is performed in a servo-hydraulic testing machine with conventional test frequency of 20 Hz and stress ratio of R = 0.1. Fatigue tests without rupture (run-outs) are stopped at $5 \cdot 10^6$ load cycles. TS 2 and TS 3 were carried out in the presented testing device with approximately 390 Hz and stress ratios of R = 0.1 and R = 0.5.

Run-outs are stopped at $5 \cdot 10^8$ load cycles, which takes 15 days of testing time. A total of 89 fatigue tests, which include the area of high and very high cycles, are conducted in order to establish the SN-curves. The influence of test frequency and stress ratio is investigated. In general, the test series give information about the occurrence of late ruptures.

3. Results of fatigue tests

3.1. General

The results of the fatigue tests are presented in the following section. The diagrams show the individual test results and the determined SN-curves with a probability of survival of 50 %. In the area of high cycles the fatigue test data is evaluated by linear regression analysis and represented by a straight line with slope m. As it can be seen in Fig. 7 and Fig. 8, the results in the transition region show only cracks up to $3 \cdot 10^6$ load cycles. The crack always initiates at the surface from the notches of the weld. A change in damage mechanism cannot be observed. For this reason, a fatigue limit is assumed for the present fatigue test data. The test results in the transition region are evaluated with the staircase method and form a horizontal asymptote. The SN-curves are represented by these two parts and have a knee point at the intersection.

3.2. Influence of test frequency

The influence of test frequency on the results of fatigue tests of steel is often considered minimal for test frequencies reaching 1000 Hz, with the circumstance as there is no corrosion, high temperature, loading at the yield strength or specimen heating [11,12]. By evaluating the influence of test frequency on the fatigue test results, the material's internal and external influences must be distinguished [13]. On the one hand, there is the internal influence of increasing strain rate at high test frequencies. An increase of strain rate may affect the plasticity at the crack tip. The crack propagation rate may be reduced, which may cause an extended fatigue life [13]. On the other hand, the external influences are high temperature, corrosion and specimen heating. In the present case, the fatigue tests are performed at room temperature and corrosion is absent. However, the specimens are heated during the fatigue test due to inner friction. The amount of specimen heating depends on the load level.

The test results of TS 1 and TS 2 are illustrated in Fig. 7. The test results of TS 1 are plotted as the numbers of cycles until rupture in contrast TS 2 plots the numbers of cycles until crack initiation. The height of the nominal stress range of TS 2 was limited because of the power amplifier. It can be seen that the results of both test series do not differ significantly in the HCF area. The SN-curve of TS 1 with a slope of $m = 3.8$ is slightly steeper in comparison to the SN-curve of TS 2 with a slope of $m = 4.1$. The calculated fatigue limit of TS 1 is 160.7 N/mm². The fatigue limit of TS 2 with 141.9 N/mm² is 11.7 % lower than the fatigue limit of TS 1. For this reason, the knee point of TS 2 is displaced at a higher number of cycles with 1,901,787 load cycles than the knee point of TS 1 with 913,750 load cycles.

In general, the comparison of fatigue tests conducted at 20 Hz and 390 Hz shows a good agreement and demonstrates that the developed testing device is qualified for fatigue tests. A significant influence of test frequency cannot be observed. The determined fatigue limit in the transition region of fatigue tests performed at 20 Hz is 11.7 % higher than the fatigue tests performed at 390 Hz. This result may be attributed to the limited number of fatigue tests in the transition region and the chosen increment between the load levels. Further fatigue tests should be carried out in order to verify this result in the transition region.

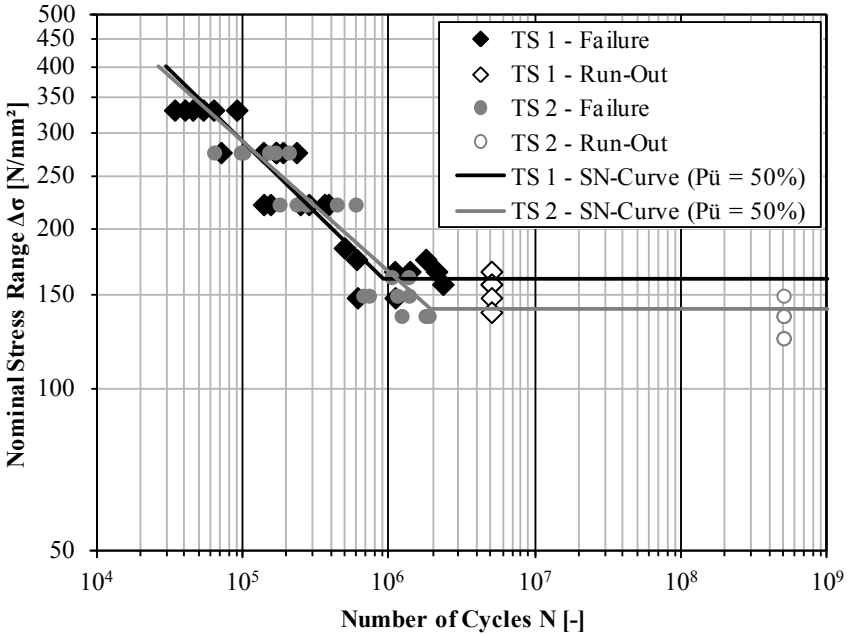

Fig. 7. Test results of TS 1 and TS 2.

3.3. Influence of stress ratio

The decrease of fatigue strength in case of welded joints in the area of very high cycles may be attributed to high tensile residual stresses [14] and the loading of torsion [15]. In the present case of small test specimens the level of residual stresses is generally assumed to be low. However, the influence of residual stresses can approximately be investigated by fatigue tests with high stress ratio of $R > 0.5$ [2]. Due to this TS 3 is performed with a stress ratio of $R = 0.5$ in order to investigate the influence of high tensile residual stresses.

The test results of TS 2 and TS 3 are illustrated in Fig. 8. The test results of both test series are plotted as numbers of cycles until crack initiation. The height of the nominal stress range of TS 3 was limited because of boundary conditions of the testing device at high mean stresses. The scatter of fatigue test results is increasing with decreasing nominal stress range. The slope of the test series is determined from fatigue test data in a region with high scatter. The results of both test series do not differ significantly in the HCF area. The SN-curve of TS 2 with a slope of $m = 4.1$ has a steeper course in comparison to the SN-curve of TS 3 with a slope of $m = 4.7$. The calculated fatigue limit of TS 2 is 141.9 N/mm². The fatigue limit of TS 3 with 140.4 N/mm² is 1.0 % lower than the fatigue limit of TS 2. The knee point of TS 3 is displaced at lower number of cycles with 1,239,512 load cycles than the knee point of TS 2 with 1,901,787 load cycles. This is caused by the difference in slope to a certain extent.

The comparison of fatigue tests conducted at $R = 0.1$ and $R = 0.5$ show a good agreement in the transition region, where a significant influence of stress ratio cannot be observed. The determined fatigue limit in the transition region of fatigue tests performed at $R = 0.1$ and $R = 0.5$ is nearly the same. The slope of the test results in the HCF regime of the lower stress ratio is steeper than the test results of the higher stress ratio. This is caused by the greater maximum load. Further fatigue tests at higher stress ratios than $R = 0.5$ should be carried out in order to simulate tensile residual stresses in the area of yield stress.

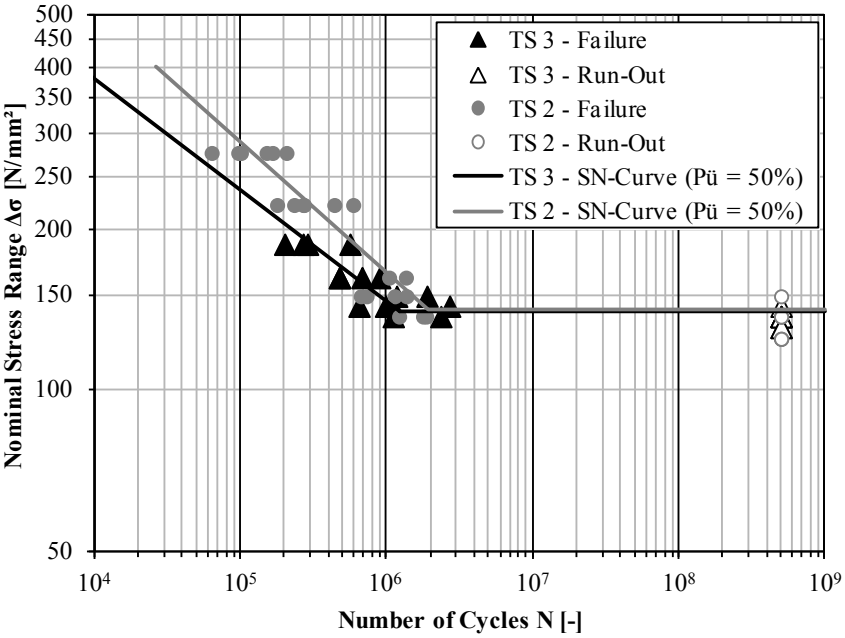

Fig. 8. Test results of TS 2 and TS 3.

4. Conclusions and Outlook

This paper presents fatigue tests on butt welded steel specimens until very high cycles applying a new testing device. The presented testing device operating by 390 Hz allows for conducting fatigue tests of butt welds reaching very high cycles in an acceptable period of time. Three test series were conducted at axially loaded butt welds. Cracks beyond $3 \cdot 10^6$ load cycles cannot be observed. All cracks started at the surface from the notches of the weld. The present fatigue data showed a fatigue limit. One test series was carried out with a servo-hydraulic testing machine at a test frequency of 20 Hz. Two further test series were carried out with the presented testing device at a test frequency of 390 Hz. The comparison of the test results conducted at test frequencies of 20 Hz and 390 Hz showed a good agreement, which demonstrates that the presented testing device is qualified for fatigue tests. A significant influence of test frequency cannot be observed in the HCF area. In the transition region the fatigue limit of the test results carried out at 20 Hz is 11.7 % higher than the fatigue limit of test results carried out at 390 Hz. This may be attributed to the limited number of fatigue tests in the transition region and the chosen distance of load levels. In order to verify the test results in the transition region further fatigue tests should be carried out. The comparison of the fatigue tests conducted at $R = 0.1$ and $R = 0.5$ illustrated that the determined fatigue limit in the transition region of fatigue tests of both test series were nearly the same. A significant influence of stress ratio respectively tensile residual stresses cannot be observed in the transition region. A further decrease of the SN-curve cannot be detected for a stress ratio of $R = 0.5$. The slope of the test results carried out at $R = 0.5$ is higher than the slope of test results carried out at $R = 0.1$. This is due to the greater maximum load. In order to simulate tensile residual stresses in the area of yield stress further fatigue tests at higher stress ratios than $R = 0.5$ should be carried out.

References

[1] Eurocode 3. Design of steel structures, part 1-9: fatigue. CEN European Committee for Standardization; 2012.
[2] Hobbacher AF. Recommendations for Fatigue Design of Welded Joints and Components. International Institute of Welding, Document IIW-1829-07 ex XIII-2151r4-07/XV-1254r-07, Welding Research Council, New York, 2009.

[3] Sonsino CM. Course of SN-curves especially in the high-cycle fatigue regime with regard to component design and safety. Int. J Fatigue 2007;29:2246-58.
[4] Pyttel B, Schwerdt D, Berger C. Very high cycle fatigue – Is there a limit? Int. J Fatigue 2011;33:49-58.
[5] Bacher-Höchst M, Berger C, Sonsino CM, Vormwald M. Current developments and trends on structural durability. Mat.-wiss. u. Werkstofftech. 2008;39:680-7.
[6] Sonsino CM, Maddox SJ, Haagensen P. A Short Study on the Form of the SN-curves for Welded Details in the High-Cycle-Fatigue Regime. IIW-Doc. No. XIII-2045-05, 2005.
[7] Hobbacher AF. The new IIW recommendations for fatigue assessment of welded joints and components – A comprehensive code recently updated. Int. J Fatigue 2009;31:50-8.
[8] Deutsches Patent 10204258.6. Prüfvorrichtung zur Dauerschwingprüfung von Prüflingen. Alt A, 2005.
[9] Schaumann P, Keindorf C, Alt A. Hochfrequente Ermüdungstests an Schweißverbindungen mit einem neu entwickelten Magnetresonanzprüfrahmen. Große Schweißtechnische Tagung, 17.-19.09.2008, Dresden, 2008.
[10] Schaumann P, Steppeler S. Ermüdungsverhalten von Schweißverbindungen von Tragstrukturen für Windenergieanlagen bei sehr hohen Lastwechselzahlen. DVS Berichte 277 - Schweißen im Schiffbau und Ingenieurbau 2011, S. 53-58, ISBN 978-3-87155-269-4, 2011.
[11] Haibach E. Betriebsfestigkeit, Verfahren und Daten zur Bauteilberechnung. 3. Auflage. Springer-Verlag Berlin Heidelberg; 2006.
[12] Radaj D, Vormwald M. Ermüdungsfestigkeit, Grundlagen für Ingenieure. 3. Auflage. Springer-Verlag Berlin Heidelberg; 2007.
[13] Tsutsumi N, Murakami Y, Doquet V. Effect of test frequency on fatigue strength of low carbon steel. Fatigue Fract Engng Mater Struct 2009;32:473-83.
[14] Sonsino CM. Über den Einfluss von Eigenspannungen, Nahtgeometrie und mehrachsigen Spannungszuständen auf die Betriebsfestigkeit geschweißter Konstruktionen aus Baustählen. Mat.-wiss. u. Werkstofftech. 1994;25:97-109.
[15] Seeger T, Olivier R. Neigung und Abknickpunkt der Wöhlerlinie von schubbeanspruchten Kehlnähten. Stahlbau 1992;61:137-42.